Soil Salinity Mapping by Multiscale Remote Sensing in Mesopotamia, Iraq

Weicheng Wu, Waleed M. Al-Shafie, Ahmad S. Mhaimeed, Feras Ziadat, Vinay Nangia, and William Bill Payne

***Abstract*—Soil salinity has become one of the major problems affecting crop production and food security in Mesopotamia, Iraq. There is a pressing need to quantify and map the spatial extent and distribution of salinity in the country in order to provide relevant references for the central and local governments to plan sustainable land use and agricultural development. The aim of this study was to conduct such quantification and mapping in Mesopotamia using an integrated, multiscale modeling approach that relies on remote sensing. A multiyear, multiresolution, and multisensor dataset composed of mainly Landsat ETM+ and MODIS data of the period 2009–2012 was used. Results show that the local-scale salinity models developed from pilot sites with vegetated and nonvegetated areas can reliably predict salinity. Salinity maps produced by these models have a high accuracy of about 82.5–83.3% against the ground measurements. Regional salinity models developed using integrated samples from all pilot sites could predict soil salinity with an accuracy of 80% based on comparison to regional measurements along two transects. It is hence concluded that the multiscale models are reasonably reliable for assessment of soil salinity at local and regional scales. The methodology proposed in this paper can minimize problems induced by crop rotation, fallowing, and soil moisture content, and has clear advantages over other mapping approaches. Further testing is needed while extending the mapping approaches and models to other salinity-affected environments.**

***Index Terms*—Multiscale remote sensing, multiyear maxima, new processing algorithm, salinity models, soil salinity.**

I. Introduction

APPROXIMATELY, 60% of the cultivated land in the Mesopotamian plain in Iraq is seriously affected by salinity [1]; 20–30% has been abandoned in the past 4000 years [1], [2]. Because of soil salinity, yield of crops, especially, wheat of nonabandoned has declined by 20–50% by 1950s [2]. But the severity and distribution of soil salinity varies with space and time [2]–[4]. In order to prioritize any remediation effort and better plan for agricultural improvements and food security, it is of prime importance for Iraqi central and local governments to understand the distribution and severity of salinity in Mesopotamia.

Soil salinity is a common form of land degradation in irrigated areas located in dryland environments [5]–[8]. The physical appearance of salinity is strongly influenced by soil properties (e.g., moisture, texture, mineral composition, and surface roughness) as well as type of vegetation cover (e.g., halophyte and nonhalophyte, salt-tolerant and nonsalt-tolerant) [5]–[8]. Remote sensing has been widely applied for mapping and assessment of soil salinity in recent decades using vegetation indices (VIs) and combined spectral response index (COSRI) [9]–[16], best band combination [17], [18], maximum likelihood and fuzzy logic-based classifications [19]–[23], principal component analysis (PCA), surface feature unmixing, and data fusion [6], [7], [24]. Predictive models have been developed for soil salinity using different regression analysis, artificial neural network (ANN), and Kriging/CoKriging techniques [9]–[16], [18], [24]–[26]. Very recently, along with vegetation indices and reflectance of certain spectral bands, evapotranspiration (ET) and land surface temperature (LST) have been used to predict salinity in salt-affected areas [16], [27]–[29].

While these and other studies demonstrate the feasibility, advantages, and potential of remote sensing to assess soil salinity, there remain certain challenges. First, although in strongly salinized areas, salt tends to concentrate on terrain surfaces and can be easily detected by conventional remote sensing tools; however, for low-to-moderate salinity ($\mathrm{salt} < 10-15\%$), spectral confusions with other different surface features may arise leading to identification failure (either overestimation or underestimation) [6], [7]; especially, when salt concentrates in subsoil, optical remote sensing is restricted [8]. Second, soil moisture, halophyte vegetation, and salt-tolerant crops such as barley, cotton, and alfalfa can modify the overall spectral response pattern of salt-affected soils, especially in the green and red bands [6], [7], [30]. Third, lands in the states of fallow, noncrop interval in-between rotations, and crop rotations tend to be interpreted as salinized areas if only soil bareness or vegetation greenness of a single image is investigated. To avoid these problems, some authors have suggested: 1) to use images acquired at the end of dry or hot season or of multiple cropping periods [7], [8], 2) to conduct regression analysis against VIs [9]–[16] and geophysical measurement [8] in combination with

Manuscript received November 14, 2013; revised July 09, 2014; accepted September 18, 2014. Date of publication October 13, 2014; date of current version January 06, 2015. This work was supported in part by the Australian Center for International Agricultural Research (ACIAR) and in part by the Italian Government. *(Corresponding author: Weicheng Wu.)*

W. Wu was with the International Center for Agricultural Research in the Dry Areas (ICARDA), 11195 Amman, Jordan. He is now an independent scientist in Choisy-Le-Roi 94600, France (e-mail: wuwc123@gmail.com).

W. M. Al-Shafie is with the GIS Division, Ministry of Agriculture (MoA), 10001 Baghdad, Iraq.

A. S. Mhaimeed is with the College of Agriculture, Baghdad University, 00964 Baghdad, Iraq.

F. Ziadat and V. Nangia are with the Integrated Water and Land Management Program (IWLM), ICARDA, 11195 Amman, Jordan.

W. B. Payne was with ICARDA, 11195 Amman, Jordan. He is now with the College of Agriculture, Biotechnology and Natural Resources (CABNR), University of Nevada, Reno, NV 89557-0221, USA.

Color versions of one or more of the figures in this paper are available online at http://ieeexplore.ieee.org.

Digital Object Identifier 10.1109/JSTARS.2014.2360411

soil sampling and analysis. These are, no doubt, useful suggestions to minimize the mentioned problems and accomplish a better mapping work. However, most of the available studies have employed single or multidate single images to assess salinity at local scale, and their approaches are not fully repeatable or extendable for regional-scale assessment due to spatial variability and diversity in climate conditions, soil properties, and land use/management. It is, therefore, essential to develop new processing methods and approaches technically operational for regional-scale salinity mapping.

The main objectives of this study are, hence, to develop an integrated methodology operational for regional salinity quantification and assessment based on the available approaches considering the above-mentioned problematic issues, to provide relevant multiscale salinity maps for Iraqi governments, and finally, to lay a foundation for the successive regional-scale tracking of salinity change trends in space and time that may provide spatial reference for the governments to understand the impacts of land management on salinization processes in Mesopotamia.

As well as for salinity assessment, remote sensing technology has also been widely applied in other dryland research. Some scientists have utilized annual maximum (peak) VIs such as Normalized Difference Vegetation Index (NDVI) [31] to compose cloud-free NDVI [32]–[35] for assessing dryland biomass [33]–[35] and land degradation [35]–[37] in the past decades. Others have used multiyear maximum (peak) and minimum (trough) NDVI and LST to derive vegetation condition index (VCI) and temperature condition index (TCI) for monitoring droughts [38]–[40]. Clearly, annual maximum VI, if applied to salinity assessment, can resolve the problems related to cloud-cover and crop rotation (crops cultivated either in spring or summer) but cannot remove that resulted from fallow state which may last a couple of years. However, multiyear maximum, if the observation period spans 3–4 years, can minimize (if cannot completely resolve) these problems. LST is associated with soil moisture and water content [41]–[44], and high LST is related to low moisture [44]. Thus, multiyear maximal LST is a promising indicator to minimize the problem related to soil moisture.

Additionally, remote sensing-based multiscale modeling has gained a momentum in regional, continental or even global scale application [34], [45], [46] to extend plot measurements to local-scale (e.g., pilot site or watershed), and then to regional- or continental-scale [34], [46]. As Farifteh *et al.* [8] and Wu *et al.* [34] explained, such multiscale modeling is in fact an upscaling procedure to extend models developed from local studies to regional-scale assessment considering the spatial variability.

From the above brief review, we reached an understanding that regional salinity mapping and assessment require integrated approaches which consider multidimensional (or multiaspect) observation and analysis from surface (e.g., vegetated and nonvegetated areas) to subsoil (within a limited depth of, e.g., <150 cm), and from multiple biophysical characterization to traditional soil sampling. We propose, hence, in this paper a "multiyear maxima and multiscale modeling" methodology for salinity quantification in Mesopotamia, Iraq.

II. Materials and Methods

A. Study Area

Mesopotamia, "the land between rivers" in ancient Greek and encompassing a surface area of about 135 000 km^2, is a typical alluvial plain between the two famous rivers, Euphrates and Tigris (Fig. 1) and the home of multiple ancient civilizations namley Sumerian, Akkadian, Babylonian, and Assyrian [4]. As an arid subtropical region, the climate is characterized by dry hot summers and cooler winters [2], [3], [29], where annual rainfall is mostly below 200 mm, of which the average is 110 mm in Baghdad and 149 mm in Basrah in the past three decades. The mean maximum and minimum temperatures are 44°C and 25.6°C, respectively, in Baghdad, 46°C and 29.15°C in Basrah in July–August, whereas they are 16.5°C and 4.8°C in Baghdad, 19°C and 8.4°C in Basrah in December–January.

As a fluviatile plain, soils are extremely calcareous (20–30% lime) alluvial silty loam or loamy silts [2], [3], typical Fluvisols in terms of WRB (the World Reference Base for Soil Resources), and mostly saline as a result of cumulative salinization in the past 6000 years [2]–[4]. Archeological evidence revealed that crop cultivation (e.g., wheat and barley) was started as early as 4000 BC in Mesopotamia [2], [4]. Due to aridity, farming is impossible if not irrigated. Irrigation increases soil moisture and crop production, nonetheless, leads to elevation of water-table or water-logging in the area where there is no drainage or draining is slow [2]–[4]. Consequently, salts accumulate in soils after evaporation and transpiration year by year. According to Jacobsen and Adams [4], salinity had already become a serious hazard in southern Mesopotamia in the late Sumerian or early Akkadian periods, e.g., around 2400–2300 BC, and led to a decline in wheat production. The proportions of wheat and barley were nearly equal in about 3500 BC but became 1 to 6 in 2400 BC in Girsu (nowadays Thi-Qar); wheat cultivation was completely abandoned after 1700 BC and land productivity declined from 2537 l/ha before 2400 BC to 897 l/ha in 1700 BC in Larsa (also in Thi-Qar) as a consequence of salinization. Salinity is hence an old problem that contributed to the breakup of ancient civilization [4]. Unfortunately, salinization has never stopped but progressively extended to the whole Mesopotamian plain to the state as described in the beginning of the paper.

As Buringh investigated [2], the most common salt in saline soils is sodium chloride (NaCl) followed by other chlorides (e.g., $CaCl_2$, $MgCl_2$, and KCl), and sulfates (e.g., $CaSO_4{\cdot}2H_2O$, $Na_2SO_4.10H_2O$, and $MgSO_4$). Saline-alkaline soils may exist locally but real alkali soils (in black) are very scarce in Mesopotamia.

B. Field Sampling Design and Data

To achieve our objectives, comprehensive observations and measurements at different scales are required. The experiment was hence designed to be conducted at three levels, i.e., plot, local (pilot site), and regional scales, corresponding to the proposed multiscale approach. Both local (pilot site)- and

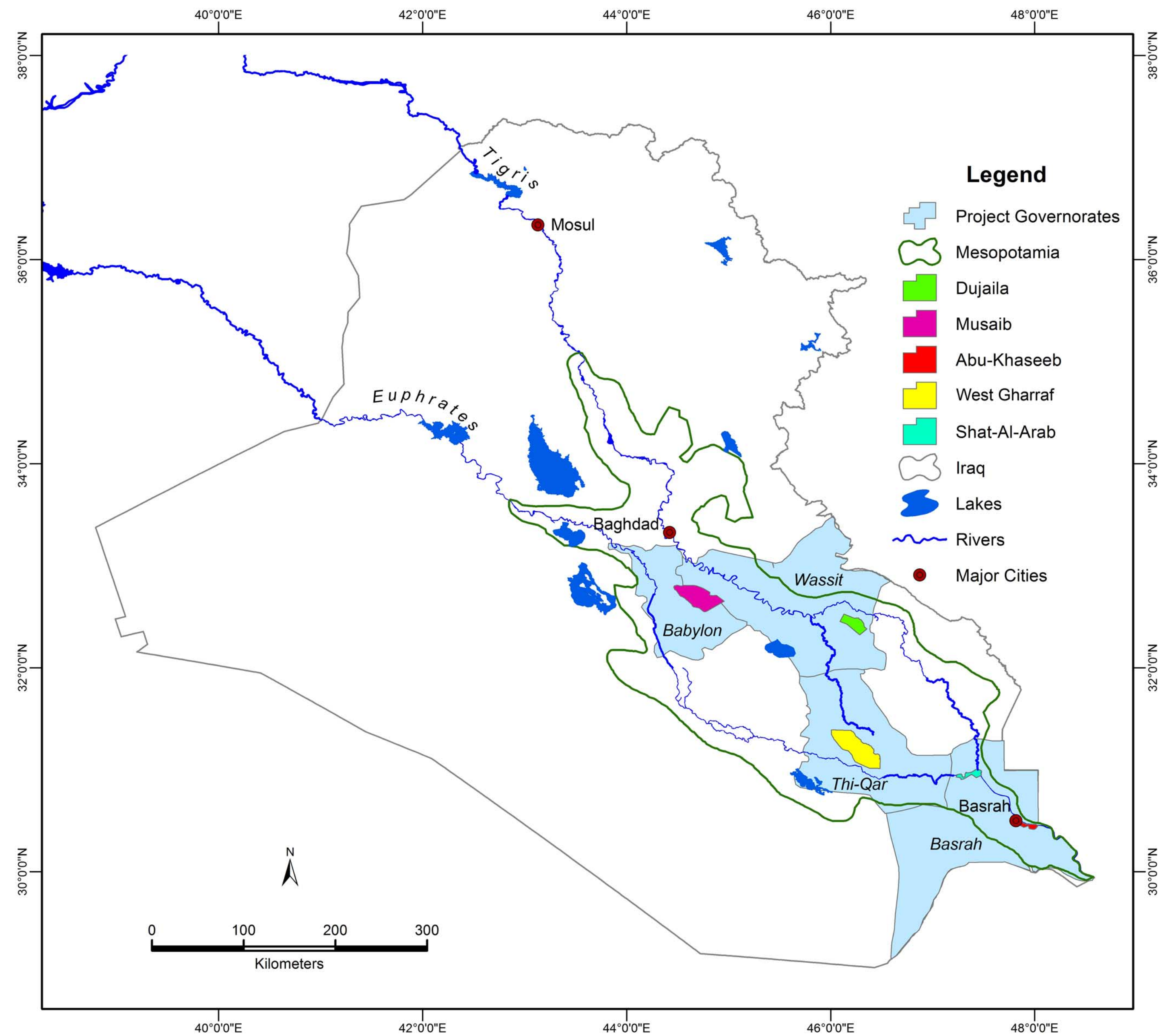

Fig. 1. Location of the five pilot sites and the whole study area, Mesopotamia, in Iraq.

regional-scale surveys were composed of plot level investigation and measurements.

Plot level survey included land use/cover investigation, crop types and performance observation (if possible), soil sampling, and apparent salinity measurement using a ground conductivity meter, EM38-MK2 (Geonics Ltd.), in an area of $1 \text{ m} \times 1 \text{ m}$. EM38 meter is capable to measure the apparent soil salinity in both horizontal (with a measurement depth up to 50 cm) and vertical (up to 150 cm) directions, of which the readings can be respectively denoted as $\mathrm{EM_H}$ (horizontal) and $\mathrm{EM_V}$ (vertical) in millisiemens per meter (mS/m). Hence, EM38 meter can reveal salinity of both surface and subsoil. However, the apparent salinity has to be calibrated by laboratory measured soil salinity. The false salinity caused by metal and/or soil moisture should be avoided while measurement is conducted.

In order to be comparable with the pixels of high-resolution satellite images such as Landsat and SPOT (e.g., 10–30 m), the survey was planned to be conducted in three plots distributed at three corners of a triangle, respectively, with a distance of about 15–20 m from each other in the same patch of land. The averaged values of the EM38 readings including both $\mathrm{EM_V}$ and $\mathrm{EM_H}$ of the three corner plots would be taken to represent the salinity of the center of the observed triangle. Soil samples for laboratory chemical analysis were to be taken from soil profiles at the depth of 0–30, 50–70, 90–110 and 120–150 cm, and from surface (0–30 cm in depth) using auger tools in the plots where EM38 was also measured.

Pilot site level survey was to serve for integrated pilot study, e.g., salinity model development and mapping at local scale. As recommended by the Iraqi government, five sites namely Musaib, Dujaila, West Gharraf, Shat-Al-Arab, and Abu

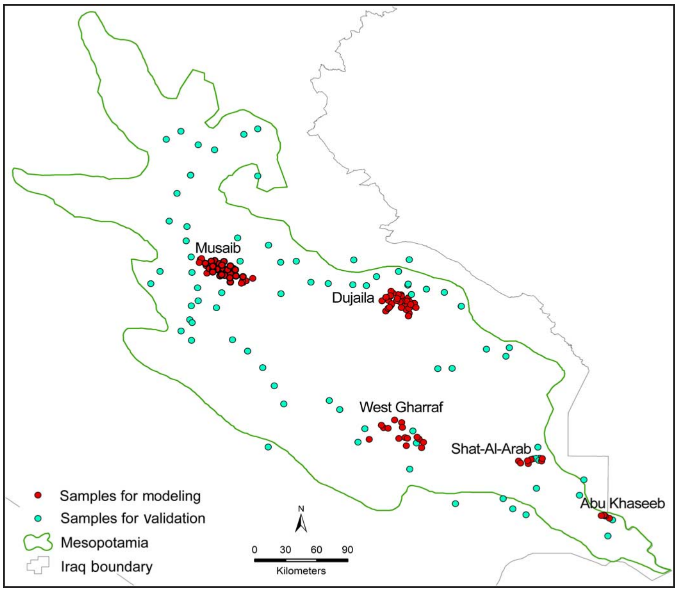

Fig. 2. Distribution of the sampling points for modeling and validation.

Khaseeb in the Mesopotamian plain (see Figs. 1 and 2 for location) were selected for pilot studies. It was planned that each pilot site should contain >5 soil profiles and >20 triangles of plots for surface survey if accessibility allowed.

Regional survey, which was aimed at salinity model development and validation at regional-scale, was to be conducted along two transects in the whole Mesopotamian Plain.

Based on the above design, field survey and sampling campaigns were conducted in the five pilot sites in the period September 2011–July 2012 and along two regional transects in Mesopotamia in April 2012 and June 2013. The sampling locations for plot level survey both in pilot sites and along the regional transects were randomly selected in the field in terms of accessibility. Due to limited budget, surface soil samples were not taken in each plot but at least in one of the three corners. Soil salinity, expressed as electrical conductivity (EC) in decisiemens per meter (dS/m), was measured in laboratory using 1:1 dilution method. In total, 187 surface soil samples (0–30 cm) with laboratory analysis and 485 pairs of EM38 measurements were obtained for this study. Sites, depths, and numbers of sampling are described in Table I.

In order to extend plot level measurements to pilot site, and then to regional-scale salinity mapping, a multiyear dataset consisting of multiresolution and multisensor satellite imagery was prepared based on the availability of images. This dataset includes 33 spring (February–April) and summer (August) Landsat ETM+ images of the period 2009–2012, four SPOT 4 images acquired in March 2010, and three RapidEye images dated April 2012, time-series of MODIS vegetation indices data (MOD13Q1), and LST (MOD11A1 and A2) from 2009 to 2012.

C. Local-Scale Modeling and Mapping

As indicated in Section I, apart from the geophysical survey by EM38 meter to understand salinity in surface and subsoil, different remote sensing indicators that can characterize the multiaspect surface biophysical features, e.g., VIs, LST, soil brightness (albedo), and principal components (PCs), need to be derived.

Instead of using one single image, a 4-year imagery dataset registered both spring and summer acquisitions, which was used to derive the multiyear maximal values of a set of VIs and nonvegetation indices (NonVIs) for each pixel. This would help avoiding some false alarm of salinity arising from fallowing, crop rotation, and variation in soil moisture. This processing can also largely remove the problem caused by the image gaps left by the Scan-Line Corrector failure (SLC-Off) in the Landsat ETM+ imagery since 2003. We assumed that it is always possible for a given piece of cropland to be cultivated in either spring or summer with normal performance in the observed period because fallow state lasts, in general, 2–3 years in Central and Southern Iraq.

Image processing in combination with field survey would allow the identification of the salt-tolerant areas, and the concentration of salt in subsoil, for example, areas with high vegetation greenness but moderate salinity as revealed by the readings of EM 38 or as measured by soil laboratory analysis. Such areas have to be defined for a specific analysis since salinity cannot be reflected by vegetation indices.

Furthermore, it is essential to separate vegetated and nonvegetated areas, as the expression of salinity in remote sensing images is different in these two types of areas. For example, the low values of VIs in nonvegetated areas (e.g., bare soil and desert) do not mean that they are all strongly salinized (high salinity). As a matter of fact, salinity is negatively correlated with VIs such as NDVI [11], [13], [28], [29], and it tends to be overestimated in the nonvegetated areas just based on VI-related models. We have to consider the integrated information from multiple spectral and thermal bands, e.g., spectral reflectance, LST, PCs, and the brightness of the Tasseled Cap transformation (TCB) [47]–[49], for salinity assessment in these areas. The rationale behind is that the spectral reflectance and its multiband linear combination (e.g., TCB and PCs) together with LST might be able to highlight the subtle difference in soil brightness (or albedo) corresponding to the difference in salinity in the nonvegetated areas.

The procedure for local-scale study in the pilot sites is presented as follows.

1) *Atmospheric correction using FLAASH model* [50] for all Landsat ETM+, SPOT, and RapidEye images.
2) *Multispectral transformation*: A set of most frequently applied VIs such as NDVI [31], SAVI (soil-adjusted vegetation index) [51], SARVI (soil-adjusted and atmospherically resistant vegetation index) [52], and EVI (enhanced vegetation index) [53] were produced from the atmospherically corrected and reflectance-based satellite imagery. We also introduced a new vegetation index in this work, the generalized difference vegetation index (GDVI) developed by Wu [54] and in the form of

$$\mathrm{GDVI} = (\rho_{NIR}^{n} - \rho_{R}^{n})/(\rho_{NIR}^{n} + \rho_{R}^{n^n}) \tag{1}$$

TABLE I
LOCATION, DEPTH, AND NUMBER OF SOIL SAMPLES AND EM38 MEASUREMENTS

Pilot sites	Number of soil profile (0–150 cm)	Number of surface soil samples (0–30 cm)			Number of EM38 readings	
		Sep. 2011–Apr. 2012	*Supplemental Jun.–Jul. 2012*	*Jun. 2013*	*Mar.–Apr. 2012*	*Supplemental Jun.–Jul. 2012*
Musaib	13	30	6		45	23
Dujaila	5	17	6		65	17
West Gharraf		22	4		57	17
Shat-Al-Arab	4	8			54	
Abu Khaseeb	5				15	
Transects						
Transect 1-North		26		13	60	
Transect 2-South		44		11	132	
Total	27		187		485	

where ρ_{NIR} is the reflectance of the near-infrared band and ρ_R is that of the red band, and n is the power, an integer from 1 to n. When $n = 1$, GDVI = NDVI. As Wu concluded [54], when $n = 2$, GDVI is better correlated with LAI (leaf area index) in all biomes, and more sensitive to low vegetal biomes than other vegetation indices. However, with the increase of n (e.g., $n = 3$ and 4), GDVI becomes saturated and insensitive to densely vegetated areas (e.g., wheat cropland, forest). High-power GDVI is thence only relevant for application in sparsely vegetated dryland biomes (such as rangeland and woodland). Our earlier studies show that GDVI is a powerful salinity indicator [28], [29], [55]. We applied this index ($n = 2$) together with others in soil salinity modeling and mapping in this study.

Regarding NonVIs, as well as NDII (normalized difference infrared index) [56], TCB, PC1, and PC2, LST were derived from Landsat ETM+ images.

3) *Derivation of the multiyear maxima of VI and nonVI images:* An algorithm using IDL language was designed for this purpose. The multiyear maxima of VIs and NonVIs of the period of 2009–2012 were derived for each pixel in all pilot sites. For NonVIs, multiyear spring maxima, i.e., the maxima during the crop growing period from February 01 to April 15 (note: barley is harvested in the end of April) were also produced.

   We have to mention that SPOT and RapidEye images do not contain any thermal band to derive LST and thus cannot be individually used for salinity modeling in our study. After resampling the pixels to 30 m, their VIs (NDVI, SAVI, and GDVI) and NonVIs (PC1 and PC2) were integrated into those of Landsat ETM+ to derive the maxima of VIs and NonVIs in each pixel.
4) *Extraction of the maxima of each VI and nonVI corresponding to the field sampling locations:* Both maximal images of VIs and NonVIs were converted into TIF format, and imported into ArcGIS to extract the maximal values corresponding to each sampling plot location.
5) *Division of the vegetated and nonvegetated areas:* A thresholding technique was applied to the multiyear-maximal NDVI to determine the threshold for division of the vegetated and nonvegetated areas followed by a mask operation.
6) *Linking multiyear maxima with plot-scale measurements:* The extracted maxima of VIs and NonVIs were coupled with their correspondingly averaged plot-level EM38 readings or laboratory-measured soil electrical conductivity using SYSTAT, a software for statistical analysis and modeling, for salinity model development using multiple linear regression analysis at the confidence level of 95%. A positive correlation between salinity and LST, PCs and TCB, and a negative correlation between salinity and different VIs, especially GDVI and NDVI, were observed.

   Two types of salinity models were obtained: a) specific salinity models for vegetated and nonvegetated areas resulted from multiple linear regression modeling that was applied to two groups of samples located in vegetated and nonvegetated areas and b) integrated salinity models in which all samples in the same pilot site were input for modeling but vegetated and nonvegetated areas were separately treated.
7) *Evaluation and application of the salinity models:* To understand whether the models obtained are operational, the specific and integrated models were, respectively, applied back to the maxima of VIs and NonVIs of the period 2009–2012 to produce local-scale salinity maps. These maps were evaluated against the ground-measured data by linear regression model [29], [34]. If the agreement between the measured and predicted salinity is $\geq 80\%$, the models developed are considered operational at local-scale and the salinity maps are reliable.

D. Regional-Scale Mapping

1) *Regional-scale modeling:* Models obtained from any pilot site cannot be directly applied to regional-scale salinity mapping due to lack of spatial representativeness. That is why we proposed here a "multiscale modeling" approach to upscale plot-level measurements

TABLE II
SALINITY MODELS FOR THE PILOT SITES AND THE WHOLE MESOPOTAMIA

Scale		Type	Salinity models	Error scope	Multiple R^2
Pilot Site scale	Musaib	Vegetated area	$EM_V = -824.134 + 918.536*GDVI - 754.204*\ln(GDVI)$	± 41.700	0.925
			$EM_H = -606.197 - 460.043*\ln(GDVI) + 245.086*Exp(GDVI)$	± 48.559	0.862
		Nonvegetated area	$EM_H = 2608853.46 + 1842.4LST - 554286.69*\ln(LST)$	± 51.217	0.846
	Dujaila	Vegetated area	EC = = −2.87 −23.27ln(GDVI) (dS/m)	± 5.240	0.874
			$EM_V = 535.403 - 487.905GDVI$	± 64.168	0.729
		Nonvegetated area	$EM_V = -2725.05 + 10.018*LST - 509.494*NDII$	± 73.23	0.650
	West Gharraf	Vegetated area	$EM_V = -78.811 - 353.217\ln(GDVI)$	± 143.992	0.684
		Nonvegetated area	$EM_V = -19337.102 + 63.795*LST$	±166.515	0.578
Regional scale		Vegetated area	$EM_V = 66.338 - 258.114*\ln(GDVI)$	± 88.882	0.717
		Nonvegetated area	$EM_V = 3055497.34 + 2161.09*LST - 649347.93*\ln(LST)$	± 92.524	0.695

Note: EM_V and EM_H can be converted into EC (dS/m) from the regional transect sampling, i.e., $EC = 0.0005EM_V^2 - 0.0779EM_V + 12.655$ ($R^2 = 0.8505$); and $EC = 0.0002EM_H^2 + 0.0956EM_H + 0.0688$ ($R^2 = 0.7911$).

and high-resolution-derived models to regional-scale assessment. To do so, the data from different pilot sites, which are situated in different locations in Mesopotamia (Fig. 2), were integrated together for regional-scale modeling using the same multiple regression model.

2) *Upscaling test and regional salinity mapping:* Since we will use MODIS data (VIs and LST) for regional salinity mapping, it is still not clear whether the models developed from high-resolution data (e.g., Landsat and SPOT) are applicable to MODIS data. For this reason, the best salinity indicators as revealed in the previous steps, the multiyear maxima of GDVI, and the LST maxima of the crop growing period from February to April in 2009–2012 (of the frame 168-37) were linked, respectively, to the multiyear maxima of MODIS GDVI (calculated from MOD13Q1), and the maximal LST (MOD11A2) of the same period after resolution degradation of the Landsat data from 30 to 250 m and upgrading of LST data from 1000 m to 250 m. This processing was aimed at minimizing the information loss or unrealistic improvement [54]. 1000 random points covering all land cover types such as barelands (deserts, bare soils, and bare rocks), saline soils, urban areas, rangeland, and croplands were generated. By removing those falling in roads and swamps, it was found that Landsat GDVI ($GDVI_L$) is strongly correlated with MODIS GDVI ($GDVI_M$) [$R^2 = 0.839$ in (2)], and the same was obtained for Landsat LST and MODIS LST [$R^2 = 0.795$ in (3)]

$$GDVI_M = 0.7837GDVI_L + 0.1665 \text{ or } GDVI_L = (GDVI_M - 0.1665)/0.7837 \quad (2)$$

$$LST_M = 0.7054LST_L + 90.496 \text{ or } LST_L = (LST_M - 90.496)/0.7054 \quad (3)$$

Therefore, with relevant adjustment of MODIS GDVI and LST in line with (2) and (3), regional models developed from high resolution Landsat data are applicable to the adjusted MODIS data for regional salinity mapping.

For such upscaling test, one may also propose the same random processing for multiple Landsat scenes against MODIS data to get the average to evaluate the extendability. Since the land cover types are the same in the region, the results should be more or less similar to what we have obtained.

3) *Validation*: The regional salinity map derived from the MODIS data was evaluated against the field samples from two regional transects (blue points in Fig. 2) to check its reliability and accuracy.

III. RESULTS AND DISCUSSION

After the above processing, both local- and regional-scale salinity models obtained are listed in Table II, and local-scale and regional-scale salinity maps are presented in Figs. 3 and 4 for discussion.

A. Salinity Models and Maps

As our test revealed in the Dujaila site [29], specific models for vegetated and nonvegetated areas were not recommended for salinity mapping due to their low reliability (e.g., $< 37\%$). Thus, what are presented in Table II are the integrated models taking all the samples into account, whereas vegetated and nonvegetated areas were separated during the multiple linear regression analysis in each pilot site. We see that among all the VIs, GDVI or its variant such as ln(GDVI) is the most representative indicator for vegetated areas, and LST (and NDII) for nonvegetated areas in all pilot sites. By the way, for sites Shat-Al-Arab and Abu Khaseeb, independent models were not developed due to limited soil sample number (8 and 5, respectively).

It is also noted that the salinity models obtained are different from each other in all pilot sites; none of them can be directly extended to regional-scale mapping due to spatial variability. However, these models can reliably predict soil salinity with an accuracy of about 82.57% in Dujaila and 83.01% in Musaib against the field measured data. Hence, they were considered operational for their respective pilot sites.

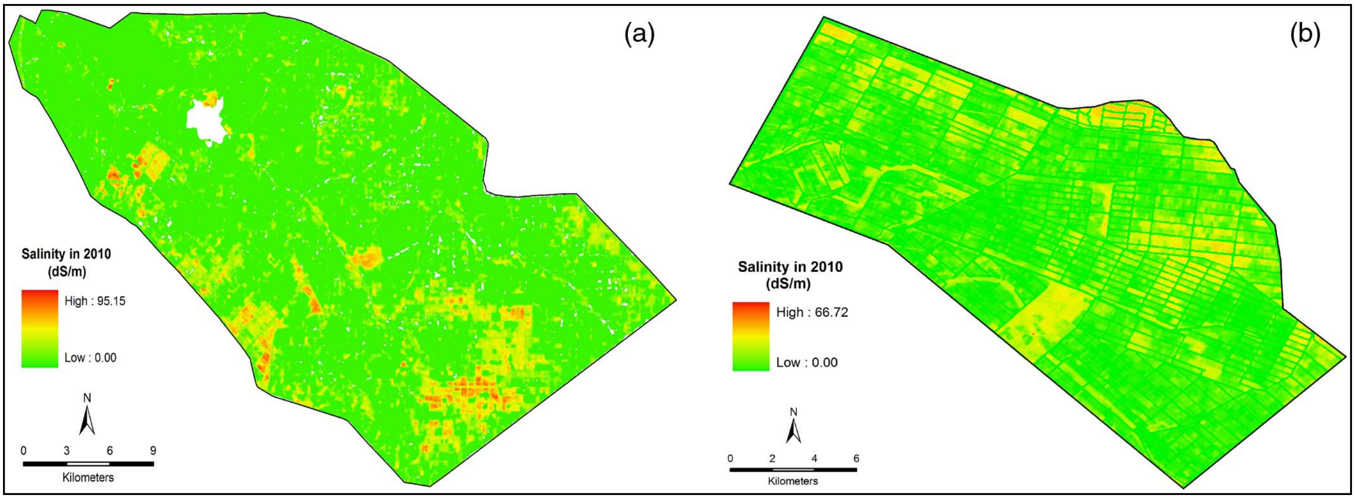

Fig. 3. Salinity of the pilot sites: (a) Musaib and (b) Dujaila.

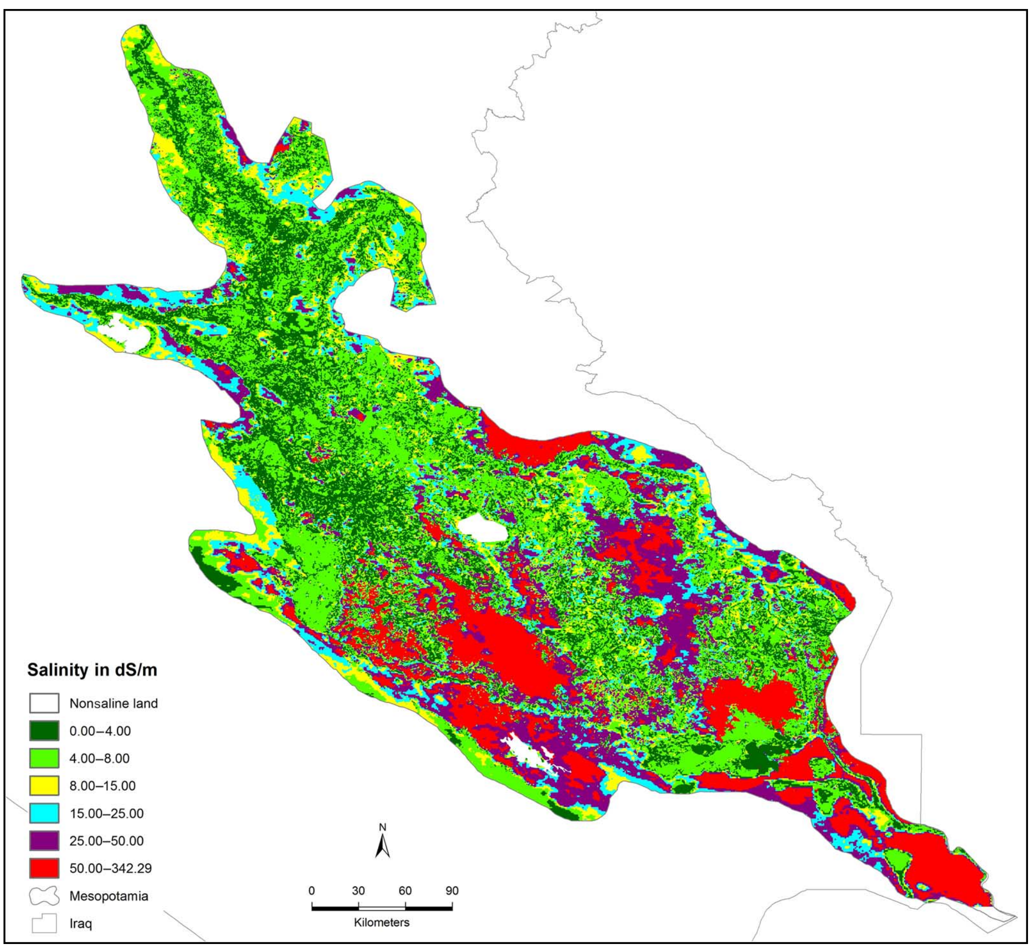

Fig. 4. Present-state salinity map of Mesopotamia (expressed in EC classes as required by users).

For the regional-scale models, the multiple correlation coefficients R^2 are relatively lower than those in pilot sites due to homogenization of samples from different pilot sites after integration; nonetheless, they have higher applicability in regional-scale mapping.

It is worth mentioning that most of the EM38 measurements in spring (March–April) 2012 did not show any promising correlation with VIs except for the Dujaila site perhaps due to the problem of soil moisture after rainfall or irrigation while measurements were undertaken in the field. For this reason, a

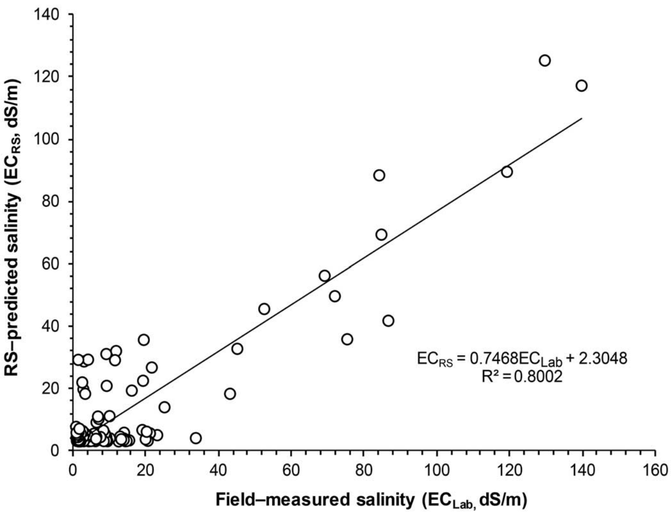

Fig. 5. Agreement of the remote sensing-predicted salinity ($\mathrm{EC_{RS}}$) versus field-measured salinity ($\mathrm{EC_{Lab}}$).

supplemental sampling campaign was carried out in the dry season after crops harvesting (June–July 2012). These EM38 readings show a good correlation with the multiyear maximal VIs and NonVIs in all pilot sites and were used for developing salinity models by multiple linear regression analysis. NDII and LST are of both vegetation and nonvegetation characters, and were included in the integrated salinity modeling for both vegetated and nonvegetated areas.

The local salinity maps of the present-state taking the sites Musaib and Dujaila as an example [Fig. 3(a) and (b)] are in a good agreement with ground data ($\mathrm{R}^2 = 0.830$ in Musaib, and 0.826 in Dujaila). We consider that these maps are reliable.

As for the regional salinity map (Fig. 4), the accuracy evaluation revealed that 23 of the 121 regional samples taken along two transects and the surface EC of 27 soil profiles in pilot sites that were not used for modeling were abnormal due to internal problem of samples, most probably, derived from laboratory analysis (because the correlation among Cl^-, Na^+, and EC is very low, e.g., $\mathrm{R}^2 = 0.047$); however, the remaining 98 samples show a good accordance with remote sensing predicted salinity. The observation accuracy is 80.9%, and the statistical accuracy of the regional salinity map obtained by linear regression analysis at the confidence level of 95% is 80.02% (Fig. 5). Therefore, the regional map presented in Fig. 4 was considered reliable.

The agreement between the measured and remote sensing predicted salinity as shown in Fig. 5 is higher in the high salinity part than low salinity one. This is probably due to the fact that coarse-resolution LST has lower sensitivity to low salinity. An overestimation of about 2–10 dS/m may occur in some places in the weakly salinized areas. However, the sensitivity to low salinity can be improved if high resolution LST data are available.

One may have concern about the reasonability to use soil surface temperature, LST, as salinity indicator which was finally retained in the models for the nonvegetated areas. As Wu *et al.* [29] argued, it is commonly known that thermal conductivity of materials is temperature (T)-dependent, and the former is associated with electrical conductivity (EC). However, the interrelationship between the thermal and electrical conductivities is complex and may change significantly depending on materials, e.g., soil types. Some authors [5]–[7] have explored the possibility to use the thermal band to identify the salt-affected soils but they have not discussed the mechanism behind. Abu-Hamdeh and Reeder [57] ascertained the relationship between thermal conductivity and salinity, and found that thermal conductivity decreases with the increase in the amount of added salts at given moisture content. Sepaskhah and Boersma [58] found that the apparent thermal conductivity is independent of water content at very low water contents. Consequently, in driest condition (at lowest moisture or water content), thermal conductivity is associated with the salt amount—salinity. We believe, therefore, that LST-based models are relevant for mapping salinity in nonvegetated areas.

Concern may also be addressed on the applicability of the models. It is clear that the models obtained from pilot sites are not recommended for direct application to similar areas for salinity mapping without relevant adaptation. Of higher representativeness, the regional-scale models can be disseminated to the similar environment for this purpose.

B. Assessment of the Integrated Processing Approach

Different from the other authors (e.g., [10], [17], and [18]), we used multiyear imagery dataset to derive the multiyear maxima of VIs and NonVIs for multiscale salinity modeling followed with an upscaling analysis. The above-mentioned problematic issues that are commonly faced in salinity mapping by remote sensing were successfully minimized, and salinity maps with high reliability were produced.

Despite a number of authors [10], [17] have conducted salinity mapping and best band combination studies, but they used single or multiple single images and did not differently treat the vegetated and nonvegetated areas. Especially, authors [17] did not take into account the nonvegetated area. Their approaches cannot avoid the influences from crop rotation/fallow, and moisture, which are often problematic in large area (or scale) mapping. Hence, our approach has evident advantages over and its uniqueness different from others.

However, some imperfection was also noted. As a matter of fact, salinity has strong spatial variability; even in a small $1 \times 1\ \mathrm{m}^2$ plot, salinity may change after each 20–30 cm interval, not to mention in the 250 m pixels of MODIS data which were used for regional-scale mapping in this study. That is to say, it is unlikely to produce a regional salinity map with an accuracy of 2–3 dS/m based on the proposed methodology. What can be done is to approach the reality as much as possible by increasing the sampling number and density with a relevant spatial distribution if both time and fund are available.

C. Problems Confronted

Though great efforts have been made, problem related to salt-tolerant vegetation has not been completely resolved yet. In the pilot sites, field sampling was well conducted and halophytes were noted. But in other areas where sampling was not covered, salinity may have been underestimated as salt-tolerant crops such as barley or other halophyte vegetation were not identified out for specific analysis. As was revealed by the experiment [3], barley has a rather strong resistance to salinity, and can still grow well with good production (1.68–1.84 tons/ha) in the field where soil salinity reaches 8–16 dS/m if fertilizer (e.g., nitrogen) is given.

The second issue is related to swamps and their surroundings, e.g., in the governorates of Thi-Qar and Basrah of Southern Iraq (Fig. 1). Moisture is almost a permanent problem for salinity mapping in these areas. Swamps can be excluded out for any salinity analysis but their surroundings are mostly moist vegetated area (locally cropland but mostly halophytes). In this mapping work, we tried to find the transitional part between moist (>345 dS/m, the false salinity as LST model loses its sensitivity with increase of moisture) and nonmoist zones (<345 dS/m), and then treated the moist part as normal water body or swamp.

The third problematic issue is related to bareland. Due to security reasons, a number of sampling plots designed in the nonvegetated areas were not accessible. There were not enough samples from bare soil for model development and salinity map validation. Thus both salinity models and maps of the nonvegetated areas should be improved when security condition improves and more field data become available.

IV. Conclusion

In spite of challenges, this study demonstrates the possibility to map and quantify the spatial distribution of the salt-affected land at regional-level based on the development of local- and regional-scale salinity models in Mesopotamia, Iraq. The validated maps we produced can be tentatively provided as a reference to decision-makers for facilitating their future land use planning in Mesopotamia. The proposed method can minimize the problems related to crop rotation/fallow practices, and soil moisture, and hence is different from other approaches. The models can be applied for multitemporal salinity mapping to track the temporal and spatial changes in the Mesopotamian plain and even in the whole country.

However, one weak point is noted, i.e., the approach cannot completely remove the influence from salt-tolerant crops such as barley, alfalfa, and cotton in the areas where no field survey was conducted. In addition, coarse resolution LST data (1000 m) is really not ideal for such quantification as spatial variability of salinity has been greatly homogenized. Merely, these issues can be sorted out or improved when new thermal data with higher resolution (e.g., 60–250 m) are available, and field accessibility is improved.

In future work, as mentioned in the introduction, ET, as one of the indicators, can be taken into account together with others. In this way, remote sensing-based salinity models will be more comprehensive and relevant for both local- and regional-scale assessments.

Acknowledgment

The study was financially supported by ACIAR (Australian Center for International Agricultural Research) and the Italian Government. The authors would like to thank Dr. M. Qadir (UNU-INWEH), Mr. A. Platonov (IWMI-Tashkent), Dr. E. Christen (CSIRO), and Dr. T. Oweis (ICARDA) for their cooperation in the early stage of the work; Dr. A. A. Hameed, Dr. H. H. Al-Musawi (Ministry of Water Resources of Iraq), and Dr. K. A. Saliem (Ministry of Agriculture of Iraq) for their cooperation in field sampling; and Ms. B. Dardar (ICARDA) for her assistance in a part of image processing.

References

[1] FAO, *Country Pasture/Forage Resource Profiles: Iraq*, Rome, FAO, 2011, 34pp.
[2] P. Buringh, *Soils and Soil Conditions in Iraq*. Baghdad, Iraq: Ministry of Agriculture of Iraq, 1960, 337pp.
[3] P. J. Dieleman, Ed., *Reclamation of Salt Affected Soils in Iraq*. Wageningen, The Netherlands: International Institute for Land Reclamation and Improvement/Wageningen Publication, 1963, 175pp.
[4] T. Jacobsen and R. M. Adams, "Salt and silt in ancient Mesopotamian agriculture," *Science*, vol. 128, pp. 1251–1258, 1958.
[5] B. Mougenot, M. Pouget, and G. Epema, "Remote sensing of salt-affected soils," *Remote Sens. Rev.*, vol. 7, pp. 241–259, 1993.
[6] J. A. Zinck, "Monitoring salinity from remote sensing data," in *Proc. 1st Workshop Eur. Assoc. Remote Sens. Lab. (EARSeL)*, Ghent University, Belgium, 2001, pp. 359–368.
[7] G. I. Metternicht and J. A. Zinck, "Remote sensing of soil salinity: Potentials and constraints," *Remote Sens. Environ.*, vol. 85, pp. 1–20, 2003.
[8] J. Farifteh, A. Farshad, and R. J. George, "Assessing salt-affected soils using remote sensing, solute modelling, and geophysics," *Geoderma*, vol. 130, no. 3–4, pp. 191–206, 2006.
[9] M. D. Steven, T. J. Malthus, F. M. Jaggard, and B. Andrieu, "Monitoring responses of vegetation to stress," in *Proc. 18th Annu. Conf. Remote Sens. Soc. Remote Sens. Res. Oper.*, U.K., 1992, pp. 369–377.
[10] M. Zhang, S. Ustin, E. Rejmankova, and E. Sanderson, "Monitoring Pacific coast salt marshes using remote sensing," *Ecol. Appl.*, vol. 7, pp. 1039–1053, 1997.
[11] P. Brunner, H. T. Li, W. Kinzelbach, and W. P. Li, "Generating soil electrical conductivity maps at regional level by integrating measurements on the ground and remote sensing data," *Int. J. Remote Sens.*, vol. 28, pp. 3341–3361, 2007.
[12] T. Zhang *et al.*, "Using hyperspectral vegetation indices as a proxy to monitor soil salinity," *Ecol. Indic.*, vol. 11, pp. 1552–1562, 2011.
[13] C. L. Wiegand, J. D. Rhoades, D. E. Escobar, and J. H. Everitt, "Photographic and videographic observations for determining and mapping the response of cotton to soil salinity," *Remote Sens. Environ.*, vol. 49, pp. 212–223, 1994.
[14] N. Fernández-Buces, C. Siebe, S. Cram, and J. L. Palacio, "Mapping soil salinity using a combined spectral response index for bare soil and vegetation: A case study in the former lake Texcoco, Mexico," *J. Arid Environ.*, vol. 65, pp. 644–667, 2006.
[15] D. B. Lobell, J. I. Ortiz-Monasterio, F. C. Gurrola, and L. Valenzuela, "Identification of saline soils with multiyear remote sensing of crop yields," *Soil Sci. Soc. Amer. J.*, vol. 71, pp. 777–783, 2007.
[16] J. A. Poss, W. B. Russell, and C. M. Grieve, "Estimating yields of salt- and water-stressed forages with remote sensing in the visible and near infrared," *J. Environ. Qual.*, vol. 35, pp. 1060–1071, 2006.
[17] R. S. Dwivedi and B. R. M. Rao, "The selection of the best possible Landsat TM band combination for delineating salt-affected soils," *Int. J. Remote Sens.*, vol. 13, pp. 2051–2058, 1992.
[18] A. A. Eldeiry and L. A. Garcia, "Comparison of ordinary kriging, regression kriging, and cokriging techniques to estimate soil salinity using Landsat images," *J. Irrig. Drain. Eng.*, vol. 136, pp. 355–364, 2010.
[19] D. W. Roberts, T. I. Dowling, and J. Walker, "FLAG: Fuzzy landscape analysis GIS method for dryland salinity assessment," CSIRO, Australia, Tech. Rep. No 8/97, 1997 [Online]. Available: http://www.clw.csiro.au/publications/technical97/tr8-97.pdf, accessed on Oct. 2013
[20] G. Metternicht, "Assessing temporal and spatial changes of salinity using fuzzy logic, remote sensing and GIS. Foundations of an expert system," *Ecol. Model.*, vol. 144, pp. 163–177, 2001.
[21] D. Malins and G. Metternicht, "Assessing the spatial extent of dryland salinity through fuzzy modeling," *Ecol. Model.*, vol. 193, pp. 387–411, 2006.

[22] W. Wu, “Monitoring land degradation in drylands by remote sensing,” in *Desertification and Risk Analysis Using High and Medium Resolution Satellite Data*, A. Marini and M. Talbi, Eds. New York, NY, USA: Springer, 2009, pp. 157–169.
[23] G. Metternicht, “Analysing the relationship between ground based reflectance and environmental indicators of salinity processes in the Cochabamba Valleys (Bolivia),” *Int. J. Ecol. Environ. Sci.*, vol. 24, pp. 359–370, 1998.
[24] R. L. Dehaan and G. R. Taylor, “Field-derived spectra of salinized soils and vegetation as indicators of irrigation-induced soil salinization,” *Remote Sens. Environ.*, vol. 80, pp. 406–417, 2002.
[25] J. Farifteh, F. van der Meer, C. Atzberger, and E. Carranza, “Quantitative analysis of salt-affected soil reflectance spectra: A comparison of two adaptive methods (PLSR and ANN),” *Remote Sens. Environ.*, vol. 110, pp. 59–78, 2007.
[26] L. Garcia, A. Eldeiry, and A. Elhaddad, “Estimating soil salinity using remote sensing data,” in *Proc. Central Plain Irrig. Conf.*, 2005, pp. 1–10 [Online]. Available: http://www.ksre.ksu.edu/irrigate/OOW/P05/Garcia.pdf, accessed on Jan. 2013.
[27] L. Garcia, A. Elhaddad, J. Chavez, and J. Altenhofen, “Remote sensing to improve ET estimates,” Presented at the *Evapotranspiration Workshop Using Best Sci. Estimate Consumptive Use*, Fort Collins, CO, USA, Mar. 12, 2010 [Online]. Available: http://ccc.atmos.colostate.edu/ET_Workshop/pdf/12_Garcia.pdf, accessed on Dec. 2012.
[28] A. S. Mhaimeed, *et al.*, “Use remote sensing to map soil salinity in the Musaib Area in Central Iraq,” *Int. J. Geosci. Geomatics*, vol. 1, no. 2, pp. 34–41, 2013, ISSN 2052–5591.
[29] W. Wu *et al.*, “Mapping soil salinity changes using remote sensing in Central Iraq,” *Geoderma Regional*, vol. 2–3, pp. 21–31, 2014, doi: 10.1016/j.geodrs.2014.09.002.
[30] B. Rao *et al.*, “Spectral behaviour of salt-affected soils,” *Int. J. Remote Sens.*, vol. 16, pp. 2125–2136, 1995.
[31] J. W. Rouse, R. H. Haas, J. A. Schell, and D. W. Deering, “Monitoring vegetation systems in the Great plains with ERTS,” in *Proc. 3rd ERTS-1 Symp., NASA SP-351*, 1973, vol. 1, pp. 309–317.
[32] B. N. Holben, “Characteristics of maximum-value composite images for temporal AVHRR data,” *Int. J. Remote Sens.*, vol. 7, pp. 1435–1445, 1986.
[33] C. J. Tucker, C. L. Vanpraet, M. J. Sharman, and G. van Ittersum, “Satellite remote sensing of total herbaceous biomass production in the Senegalese Sahel: 1980-1984,” *Remote Sens. Environ.*, vol. 17, pp. 232–249, 1985.
[34] W. Wu, E. De Pauw, and U. Hellden, “Assessing woody biomass in African tropical savannahs by multiscale remote sensing,” *Int. J. Remote Sens.*, vol. 34, pp. 4525–4529, 2013.
[35] W. Wu, E. De Pauw, “Policy impacts on land degradation: Evidence revealed by remote sensing in western Ordos, China,” in *Land Degradation and Desertification: Assessment, Mitigation and Remediation*, P. Zdruli *et al.*, Eds. New York, NY, USA: Springer, 2010, pp. 219–232.
[36] J. Evans and R. Geerken, “Discrimination between climate and human-induced dryland degradation,” *J. Arid Environ.*, vol. 57, no. 4, pp. 535–554, 2004.
[37] W. Wu, E. De Pauw, and C. Zucca, “Use remote sensing to assess impacts of land management policies in the Ordos rangelands in China,” *Int. J. Digit. Earth*, vol. 6, Suppl. 2, pp. 81–102, 2013.
[38] F. N. Kogan, “Application of vegetation index and brightness temperature for drought detection,” *Adv. Space Res.*, vol. 11, pp. 91–100, 1995.
[39] F. N. Kogan, “Global drought watch from space,” *Bull. Amer. Meteorol. Soc.*, vol. 78, pp. 621–636, 1997.
[40] Y. Bayarjargal *et al.*, “A comparative study of NOAA–AVHRR derived drought indices using change vector analysis,” *Remote Sens. Environ.*, vol. 105, pp. 9–22, 2006.
[41] R. R. Gillies and T. N. Carlson, “Thermal remote sensing of surface soil water content with partial vegetation cover for incorporation into climate models,” *J. Appl. Meteorol.*, vol. 34, pp. 745–756, 1995.
[42] J. D. Kalma, T. R. McVicar, and M. F. McCabe, “Estimating land surface evaporation: A review of methods using remotely sensed surface temperature data,” *Surv. Geophys.*, vol. 29, no. 4–5, pp. 421–469, 2008.
[43] C. R. Hain, J. R. Mecikalski, and M. C. Anderson, “Retrieval of an available water-based soil moisture proxy from thermal infrared remote sensing. Part I: Methodology and validation,” *J. Hydrometeorol.*, vol. 10, pp. 665–683, 2009.
[44] H. Qiu. (2006). *Thermal Remote Sensing of Soil Moisture: Validation of Presumed Linear Relation Between Surface Temperature Gradient and Soil Moisture Content* [Online]. Available: http://people.eng.unimelb.edu.au/jwalker/theses/HuangQui.pdf, accessed on Aug. 2013.
[45] N. C. Coops and R. H. Waring, “The use of multiscale remote sensing imagery to derive regional estimates of forest growth capacity using 3-PGS,” *Remote Sens. Environ.*, vol. 75, pp. 324–334, 2001.
[46] I. Chaubey, K. Cherkauer, M. Crawford , and B. Engel, “Multiscale sensing and modeling frameworks: Integrating field to continental scales,” *Bridge*, vol. 41, pp. 39–49, 2011.
[47] R. J. Kauth and G. S. Thomas, “The Tasseled cap—A graph description of the spectral-temporal development of agricultural crops as seen by Landsat,” in *Proc. 2nd Int. Symp. Mach. Process. Remote Sens. Data*, Purdue University, West Lafayette, IN, USA, 1976, pp. 4B41–4B51.
[48] E. P. Crist and R. C. Cicone, “Application of the tasseled cap concept to simulated thematic mapper data,” *Photogramm. Eng. Remote Sens.*, vol. 50, pp. 343–352, 1984.
[49] C. Huang, B. Wylie, L. Yang, C. Homer, and G. Zylstra, “Derivation of a tasseled cap transformation based on Landsat 7 at-satellite reflectance,” *Int. J. Remote Sens.*, vol. 23, pp. 1741–1748, 2002.
[50] M. W. Matthew *et al.*, “Status of atmospheric correction using a MODTRAN4-based algorithm,” in *Proc. SPIE Algor. Multispectral Hyperspectral Ultraspectral. Imagery VI*, 2000, vol. 4049, pp. 199–207.
[51] A. R. Huete, “A soil adjusted vegetation index (SAVI),” *Remote Sens. Environ.*, vol. 25, pp. 295–309, 1988.
[52] Y. J. Kaufman and D. Tanré, “Atmospherically resistant vegetation index (ARVI) for EOS-MODIS,” *IEEE Trans. Geosci. Remote Sens.*, vol. 30, no. 2, pp. 261–270, Mar. 1992.
[53] A. R. Huete, H. Q. Liu, K. Batchily, and W. van Leeuwen, “A comparison of vegetation indices global set of TM images for EOS-MODIS,” *Remote Sens. Environ.*, vol. 59, pp. 440–451, 1997.
[54] W. Wu, “The generalized difference vegetation index (GDVI) for dryland characterization,” *Remote Sens.*, vol. 6, pp. 1211–1233, 2014.
[55] W. Wu *et al.*, “Salinity modeling by remote sensing in central and southern Iraq,” presented at *Fall Meeting, AGU*, San Francisco, CA, USA, Dec. 3–7, 2012, Abstract B53H-07 [Online]. Available: http://abstractsearch.agu.org/ meetings/ 2012/ FM/ sections/B/sessions/B53H/abstracts/B53H-07.html
[56] M. A. Hardisky, V. Klemas, and R. M. Smart, “The influences of soil salinity, growth form, and leaf moisture on the spectral reflectance of Spartina alterniflora canopies,” *Photogramm. Eng. Remote Sens.*, vol. 49, pp. 77–83, 1983.
[57] N. H. Abu-Hamdeh and R. C. Reeder, “Soil thermal conductivity effects of density, moisture, salt concentration, and organic matter,” *Soil Sci. Soc. Amer. J. (SSSAJ)*, vol. 64, pp. 1285–1290, 2000.
[58] A. R. Sepaskhah and L. Boersma, “Thermal conductivity of soils as a function of temperature and water content,” *Soil Sci. Soc. Amer. J. (SSSAJ)*, vol. 43, no. 3, pp. 439–444, 1979.

Weicheng Wu received the B.Eng. and M. Eng. degrees in earth sciences from the East China Geological Institute, Fuzhou, Jiangxi, China, in 1986 and 1995, respectively, DESS (eq. to M. Eng.) degree in environmental engineering from the University of Paris XI (Paris-Sud), Orsay, France, in 1998, and the Ph.D. degree in geography with specialization in environmental geomatics (including remote sensing, GIS, and spatial analysis) from the University of Paris I (Panthéon-Sorbonne), Paris, France, in 2003.

In addition to his 11 years of university teaching and research experience in China, he has gained 16 years of international experience in monitoring environmental changes and problems assessment, and land resources investigation by remote sensing and GIS in Europe (France, Belgium, and Italy) and in the Middle East. From 2005 to 2007, he was a Remote Sensing Expert at NRD, University of Sassari, Sassari, Italy, and from 2007 to 2014, Remote Sensing Specialist with ICARDA (International Center for Agricultural Research in the Dry Areas), Amman, Jordan. He is currently an independent scientist in Choisy-Le-Roi 94600, France.

He has played an active role, and partly coordinated and led in 24 national and international cooperation research projects in China, France, Belgium, and Italy and at ICARDA. He has published in total 63 scientific and technical papers, of which 32 are peer-reviewed and 31 are nonpeer-reviewed conference/symposium papers. He serves as Reviewer for more than 12 ISI-refereed and nonrefereed journals in remote sensing and geography.

His research interests include land characterization such as land use/cover mapping, multitemporal and time-series change tracking, biomass and carbon sequestration/emission analysis, land degradation assessment, water resources accounting, crop production estimation, human–environmental interaction, and impacts of climate change on water resources and food security.

Waleed M. Al-Shafie was born in Baghdad, Iraq, in 1970. He received the B.S. and M.S. degrees in agricultural science, soil, and water resources from the University of Baghdad, Iraq, in 1994 and 2010, respectively.

From 2000 to 2003, he was an Assistant Researcher with IPA Agricultural Research Center, Department of Soil and Water, and from 2003 to 2007, Head of GIS Section, Ministry of Agriculture, Baghdad, Iraq. Since 2010, he has been in charge of the Manage—Planning and Follow-up Office of the AgroEcological Zoning (AEZ) Department, Ministry of Agriculture in Baghdad, and responsible for the implementation of land suitability maps for main crops in Iraq, while contributing to the development of the AEZ database which includes information of climate, soils, agricultural crops, and socioeconomic parameters for Iraq. His research interests include application of geographic information systems (GIS) and remote sensing for AEZ mapping, land suitability analysis, and salinity quantification.

Ahmad S. Mhaimeed received the B.S. degree in soil science from Baghdad University, the M.S. degree in soil survey and classification from the University of Nebraska–Lincoln, Lincoln, NE, USA, and the Ph.D. degree in soil survey from Colorado State University, Fort Collins, CO, USA.

Of 30 years of academic experience, he is currently a Full-time Professor in Soil Survey and Land Management, and Head of the Desertification Control Department, College of Agriculture, Baghdad University, Baghdad, Iraq. He has presented many papers in national and international conferences and has published 3 books and more than 70 scientific papers. His research interests include soil survey and management using GIS and remote sensing.

Feras Ziadat received the M.Sc. degree in soil conservation from the University of Jordan, and the Ph.D. degree in application of GIS and remote sensing for land use planning in arid areas from Cranfield University, U.K.

After his Ph.D., he worked with the University of Jordan as Associate Professor in Land Resource Management, GIS and remote sensing for 8 years. He currently works as a Soil Conservation and Land Management Specialist with the Integrated Water and Land Management Program, ICARDA. He has published over 44 refereed journal and conference proceedings in the area of land and water resources management. His research interests include sustainable land resource management and environmental modeling and monitoring with emphasis on the application of GIS and remote sensing on soil-landscape modeling and digital soil mapping, integrated and participatory land use planning and land evaluation, land degradation and desertification, land use changes, and integrated watershed management.

Vinay Nangia received the Ph.D. degree in water resources science and two M.S. degrees, one in biosystems and agricultural engineering and the other in geographic information science, all from University of Minnesota, Minneapolis, MN, USA.

He is an Agricultural Hydrologist with the International Center for Agricultural Research in the Dry Areas (ICARDA), Amman, Jordan. During a 9-year Postdoctoral research career, he has served as a PI of co-PI on research projects worth about 5.75 million, and authored or coauthored 59 technical publications that include 22 refereed journal articles in national or international journals. He is an internationally recognized authority in hydrologic and water quality modeling and GIS applications in water resources management. He has offered more than 20 trainings (covering a total of 400 participants) on hydrologic modeling in 10 countries. He has served as Research Advisor/Committee Member to M.S. and Ph.D. students and was a Visiting Assistant Professor (2007–2011) with the Institute of Soil and Water Conservation, Chinese Academy of Science, Beijing, China, where he co-advises graduate students. Previously, he was a NSERC Visiting Fellow with Agriculture and Agri-Food Canada conducting research on GHG emissions from sub-surface tile-drained croplands of Eastern Ontario prior to which he was a Postdoctoral Fellow with the International Water and Management Institute (IWMI), where he started his career in 2005.

Dr. Nangia serves on the Editorial Board of professional society journals.

William Bill Payne received the B.A. degree in chemistry from Wabash College, Crawfordsville, IN, USA, in 1981, and the M.S. and Ph.D. degrees in soil science from the Texas A&M University, College Station, TX, USA, in 1988 and 1990, respectively.

He is the recently appointed Dean of the College of Agriculture, Biotechnology and Natural Resources and Director of the Nevada Agricultural Experiment Station,University of Nevada Reno, Reno, NV, USA. From 2012 to 2014, he worked as Director of a $150 million CRP1.1 research program with ICARDA (International Center for Agricultural Research for the Dry Areas), Amman, Jordan, aimed at improving food security and livelihoods in the dry areas of the world. Prior to this, he served as a Professor of Crop Physiology with Texas A&M University, College Station, TX, USA, and is a former Research Director of the Norman Borlaug Institute for International Agriculture.

He has published 11 books and book-chapters, 53 refereed journal papers, and more than 100 nonrefereed conference abstracts and proceedings papers.

Dr. Payne has been named Fellow of five international scientific societies and has held numerous leadership roles at the state, national, and international levels.